Polymer Testing 132 (2024) 108388

Contents lists available at ScienceDirect

Polymer Testing

journal homepage: www.elsevier.com/locate/polytest

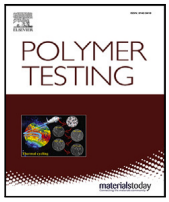

Compression testing of EPP bead foams in a vacuum chamber: Experimental investigation on the influence of the cell gas

J. Meuchelböck [a], I. Koch [b], B. Grüber [b], M. Müller-Pabel [b], M. Gude [b], H. Ruckdäschel [a,*]

[a] University of Bayreuth, Universitätsstrasse 30, Bayreuth 95447, Germany
[b] TUD Dresden University of Technology, Institute of Lightweight Engineering and Polymer Technology, Holbeinstr. 3, Dresden 01307, Germany

ARTICLE INFO

Keywords:
Mechanical testing
Compression testing in vacuum
Bead foam
Polymer
Energy absorption
Cell gas

ABSTRACT

In this study, we systematically investigate the compression behavior of Expanded Polypropylene (EPP) bead foams using precise experiments in a custom-designed vacuum chamber. The material's response is examined under controlled pressure conditions, including compression tests at both ambient pressure and 4 mbar, at various strain rates. Considering that most foams consist of more than 90% air, our focus is on elucidating the influence of cell gas on mechanical properties, such as compression modulus, plateau stress, plateau slope, and energy absorption. The impact of cell gas on recovery behavior was analyzed by loading–unloading-steps in the vacuum chamber. Notably, the presence of cell gas shows a pronounced effect on the foam's deformation behavior, particularly in the plateau region, significantly affecting its resistance to deformation and energy absorption. The findings offer valuable insights for the development of foam materials and structures/components made of foams, especially in applications where resilience and durability are paramount.

1. Introduction

Polymer bead foams have captured significant interest due to their unique combination of easy processing, the capability to produce complex parts, and their potential for lightweight applications. This combination of favorable processability and exceptional material properties has led to diverse applications in packaging, thermal insulation, sportswear, automotive components, and sandwich cores [1–7]. Expanded Polypropylene (EPP) has attained a market share of $438 million in 2023, with forecasts anticipating an increase to $620 million by 2028 [8]. The strategic development and large-scale production of these widely used material has significant economic and environmental implications. A deep understanding of the complex interplay between material, foam topology and the resulting product performance is required. Understanding the mechanical properties is crucial and can even have a decisive impact on the safety of people, as Castiglioni et al. [2] show in the context of head protection.

Polymer foams often consist of more than 90% entrapped air, offer excellent thermal insulation and deformation properties, like a unique strain-dependent energy absorption [9]. Classified into open and closed cell types, these foams differ in their response to compression and show [10]. Comparative FEA modeling indicates that in closed cell foams, the influence of cell gas on compression is more pronounced than in open cell foams [11]. In this context, Mills et al. theoretically predicted that the influence of cell gas during compression reaches its maximum at the onset of densification strain before decreasing at further compression [11,12]. Their model of the contribution of the cell gas is visualized in Fig. 1.

Ashby describes the mechanical response as an interaction of the base material, the cell structure, and the relative density [13]. Based on these considerations, the models developed by Ashby and Gibson aim to predict compression properties as a function of relative density (density of foam ρ^* divided by density of solid ρ_s), material distribution within cell walls and edges, denoted ϕ, relative modulus (foam modulus E^* divided by the solids modulus E_s) and the Poisson's ratio (ν^*) of the foam. These models are used to distinguish between brittle, plastic–elastic, and elastic foams, and between open- and closed-cell configurations. Consequently, the pressure difference between outside (p_{at}) and inside of the cells (p_0) influences the deformation behavior. Using the equations established by Ashby and Gibson, one can calculate the compression modulus (E^*) and the elastic stress (ϵ_{el}) of foams. An example using the equations for an elastic closed-cell foam illustrates that cell gas has a minor impact on the compression modulus (see

* Corresponding author.
E-mail address: ruckdaeschel@uni-bayreuth.de (H. Ruckdäschel).
URL: https://www.polymer-engineering.de/ (H. Ruckdäschel).

https://doi.org/10.1016/j.polymertesting.2024.108388
Received 18 December 2023; Received in revised form 9 February 2024; Accepted 29 February 2024
Available online 1 March 2024

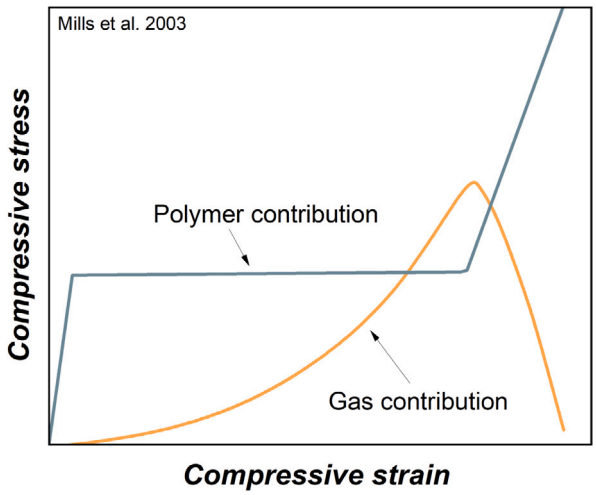

Fig. 1. Visualization of the theoretical contribution of entrapped cell gas during the compression of closed cell foams [11].

Eq. (1)) and the plateau stress (see Eq. (2)) [13].

$$\frac{E^*}{E_S} \approx \phi^2 \left(\frac{\rho^*}{\rho_s}\right)^2 + (1-\phi)\frac{\rho^*}{\rho_s} + \frac{p_0(1-2\nu^*)}{E_s(1-\frac{\rho^*}{\rho_s})} \tag{1}$$

$$\frac{\epsilon_{el}}{E_S} \approx 0.05 \left(\frac{\rho^*}{\rho_s}\right)^2 + \frac{p_0 - p_{at}}{E_s} \tag{2}$$

It is crucial to acknowledge that the equations may not fully encompass the influence of cell gas on foam deformation. Modeling the complex dynamics of diffusion processes and the increased damage to cell faces during deformation, affecting gas flow, poses a significant challenge [10–12]. The impact of cell gas becomes more pronounced after the plateau stress in the plateau region, as illustrated in Fig. 1. While these equations specifically address key parameters (E^*, ϵ_{el}) before this phase, they do not capture the deformation behavior during compression in the plateau region. Furthermore, bead foams, characterized by a unique cellular structure formed through a multi-step production process, markedly differ from conventional polymer foams, resulting in complex and hierarchical micro-, meso-, and macro-structures which influences the short- and longterm deformation behavior [14–17].

To investigate how bead foam production affects properties, Beverte conducted static compression tests on EPP in x, y, and z directions across various densities. Findings revealed that compression modulus increases with density. At the highest density (84 kg/m^3), anisotropy in the compression modulus was evident, but it was not significant in lower densities (23–57 kg/m^3). Across all densities, anisotropic behavior was noted in the plateau region, linked to the foam's structure and processing characteristics [18].

Different morphologies result in distinct response which is shown by Morton et al. They investigated the effect of cell structure on the influence of strain rate and temperature on the stress–strain behavior of two EPP foams with similar density but different microstructure. Foam A with smaller cell size (19.1 voids/mm^2) shows over 40% higher collapse stress under quasi-static conditions compared to Foam B (8.1 voids/mm^2). Collapse stress increases by 45% (Foam A) and 57% (Foam B) at a strain rate of 10^0 s^{-1} compared to quasi-static loading 10^{-3} s^{-1}. Temperature has also a huge impact and the collapse stress rises 110% at −30 °C and drops 50% at 60 °C. The influence of temperature must be taken into account during use and therefore plays an important role in product development [5].

In addition, the cellular structure of bead foams is also influenced by density. Rumianek et al. demonstrated that an increase in foam density of EPP results in altered cell structures, indicated by greater strut thickness, consequently leading to improved resistance against compression. This phenomenon was observed consistently across various deformation rates, where higher strain rates corresponded to elevated compression modulus at the same density, and higher density led to higher compression modulus [4].

Viot et al. studied the change in morphology during dynamic compression tests and compared microtomographic images after each impact. They observed instead of the expected correlation between bead density and deformation, a more complex deformation behavior. In conclusion, the most porous beads of the welded sample create zones of weakness that lead to local collapse, which is transmitted to neighboring beads [19].

In a complementary study, Viot investigated the hydrostatic compression of EPP using a flywheel and a hydrostatic chamber. By varying strain rates and densities, he observed unexpected nonlinear elasticity and transverse isotropy during hydrostatic loading, in contrast to the expected isotropic behavior observed in uniaxial compression. These changes are attributed to complicated interactions between the structure of the foam, the trapped gas in the microstructure, and manufacturing-induced microstructural variations [20].

Bouix et al. examined the effects of strain rates (in the range of 10^{-2} to 10^3 s^{-1}) and foam density (from 35–150 kg/m^3) on the compression properties of EPP foams. As expected, they found that higher densities show increased collapse stress, while higher strain rates consistently lead to increased collapse stress regardless of foam density. The researchers suggested that accelerated strain rates could trap cell gas in the foam due to rapid deformation. Underwater imaging confirmed that less gas escapes at higher strain rates [21].

In summary, understanding how cell gas affects bead foam compression is crucial for advancing foam development and engineering. While extensive theoretical discussion on the impact of cell gas exists, the lack of a precise experimental results hinders insights. Theoretical models suggest significant effects of the cell gas on the deformation behavior of foams, yet experimental confirmation for bead foams is lacking. This gap between theory and practice underscores the need for experimental studies to refine modeling and optimize bead foam design.

Our study aims to close this gap, by developing an innovative method to experimentally test bead foams under vacuum conditions. This approach allows us to precisely quantify the influence of air within bead foams. Moreover, it opens avenues for future studies to compare results under various pressure conditions, providing valuable insights into the complex interplay of cell gas and bead foam mechanics.

2. Experimental methodology

2.1. Material

For all performed tests, we used commercially available EPP beads (Neopolen P9230k, BASF SE) to produce plates with dimensions of 200 × 190 × 40 mm with a steam chest moulding machine (Energy foamer 5.0, Kurtz Ersa Gmbh). To avoid density inhomogeneities due to the fabrication process we cut samples from the foam boards and remove the skin [22]. Therefore we used a hollow drill with a diameter of 20 mm. The samples were cut out of the middle to a height of 20 mm with a 3D printed mold and a sharp knife. The process is visualized in Fig. 3.

To assure parallel and plain surfaces the height of each sample was measured at three different positions. After conditioning at 25 °C and 50% rel. humidity for at least seven days the geometric density of every sample was measured. The mass (m) and the volume (V) was determined and the density ρ was calculated. As a case study here EPP with a density of 60 kg/m^3 is uniformly used for all experiments.

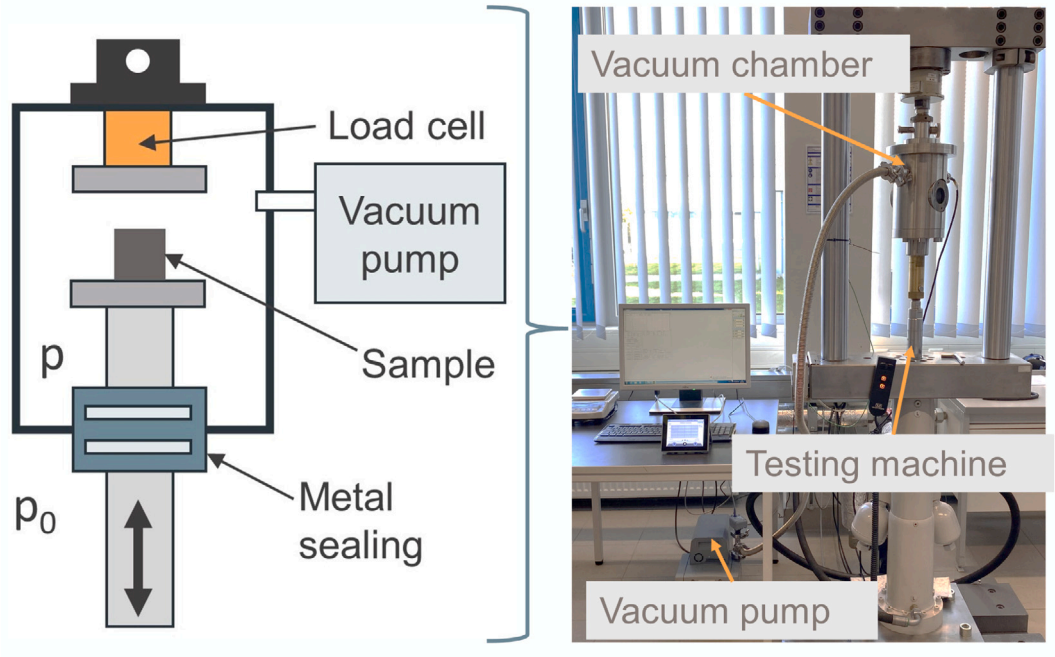

Fig. 2. Schematic representation of the vacuum chamber used (left) and installed in a servo-hydraulic testing machine (right).

2.2. Vacuum testing setup

The schematic representation of the vacuum chamber used in our experiments is depicted in Fig. 2. This chamber is integrated in a servo-hydraulic testing machine (Schenk AG, Germany) for precise testing. Displacement measurements were carried out using a position sensor attached to the piston. To eliminate any potential distortion caused by frictional forces from the metal seal, a 10 kN load cell (HBM, Germany) was positioned inside the vacuum chamber. Control over the chamber's internal pressure was achieved using a four-stage membrane vacuum pump (Vacuubrand, Germany) equipped with continuous pressure monitoring.

2.3. Development of reproducible and repeatable vacuum tests

Prior to vacuum testing, it is essential to determine the necessary evacuation time and ensure that the material remains undamaged during the evacuation process.

The evacuation process entailed continuous evacuation, followed by a designated vacuum holding time. In the pursuit of determining the optimal conditioning time for the chosen material under 4 mbar pressure, a series of compression tests were conducted after exposure periods of 24, 48, 72, and 96 h at 4 mbar and a strain rate of 1.6 s^{-1}. The obtained results were compared and a fixed conditioning time for subsequent tests was deduced.

To evaluate the impact of evacuation on foam mechanics, we first subjected specimens to a 72-hour vacuum treatment, then exposed them to 72 h of ambient conditions. We compared their mechanical performance at ambient conditions with specimens that remained in ambient conditions throughout.

2.4. Methods for analyzing the influence of cell gas

To investigate the influence of cell gas on the deformation behavior of EPP, compression tests were carried out in accordance with DIN EN ISO 844 standard. A consistent pre-force of 3 N was uniformly applied to all tests. The key parameters were analyzed via the approach and Python script of Albuquerque et al. This script calculates the densification strain based on maximum energy absorption efficiency,

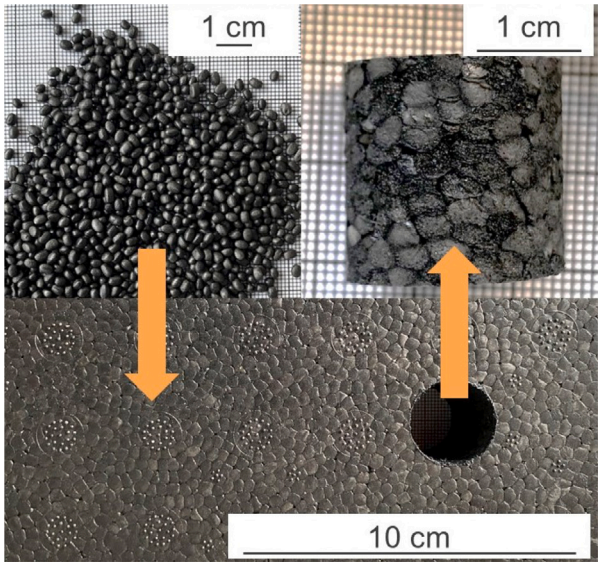

Fig. 3. Test sample production from beads, to welded plate and to the extracted test sample.

while the plateau slope indicates the slope of the optimal linear fit between plateau onset and densification strain [23,24]. To evaluate the recovery effect during unloading, we conducted an unloading step at the same testing speed. Furthermore, we systematically assessed the performance of the vacuum chamber at higher test speeds, employing three distinct strain rates: 0.016, 1.6, and 16 s^{-1}. The testing speed was determined using the formula $v(t) = \dot{\varepsilon} \cdot h_0$, where h_0 describes the initial height of each sample prior to testing. For each strain rate and pressure level, at least three samples were tested.

3. Results and discussion

In this chapter, the systematic procedure for vacuum foam testing, using EPP with a density of 60 kg/m^3 as a case study, is highlighted.

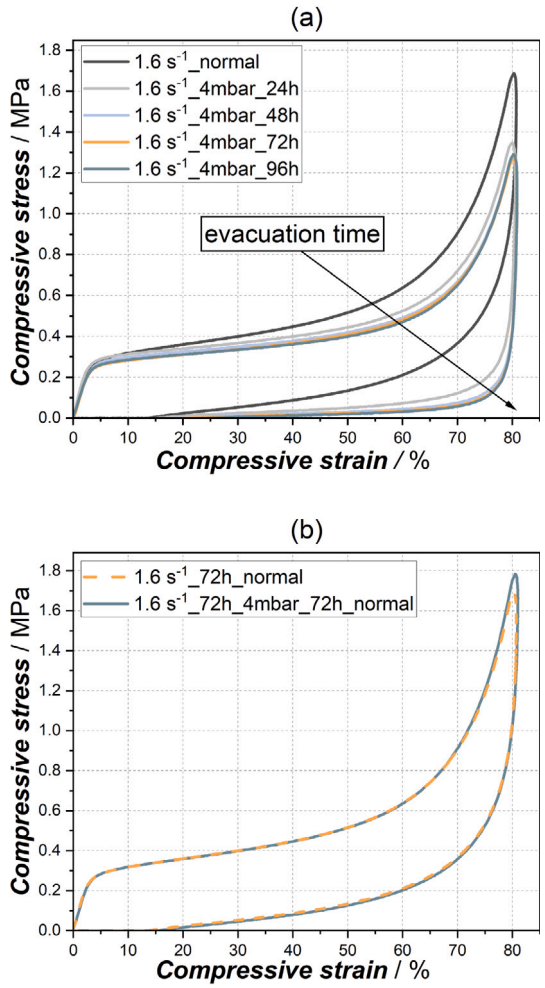

Fig. 4. Mechanical behavior of EPP (60 kg/m^3 density) at a strain rate of 1.6 s^{-1}: (a) shows the varied mechanical responses due to different evacuation times; (b) compares compressive stress–strain curves at ambient conditions between a sample conditioned for 72 h at 4 mbar, followed by 72 h at ambient pressure, and a sample without evacuation.

3.1. Optimum evacuation time and its damaging influence on EPP

Starting with analyzing the required conditioning time at 4 mbar, Fig. 4a illustrates the results obtained by varying the evacuation time. Analysis of compressive stress–strain curves shows strong differences at different conditioning times. Prolonging the evacuation period accentuates these differences compared to compression tests under ambient pressure. However, the difference become less pronounced, between 72 h and 96 h. Consequently, a 72-hour conditioning time has been selected for subsequent tests.

To assess the impact of evacuation on mechanical properties, we compared a sample evacuated for 72 h and subsequently conditioned at lab condition for 72 h with a sample stored only for 72 h under lab conditions without evacuation. The compressive stress–strain curves, illustrated in Fig. 4b, reveal that evacuation has no discernible influence on the mechanical properties.

It is crucial to note, when testing in vacuum, that the conditioning time and the effects of evacuation vary depending on the foam material and its density.

3.2. Influence of cell gas on the compression behavior of EPP

Fig. 5 provides a visual comparison between compressive stress–strain curves (Fig. 5a) and of their corresponding properties under ambient and vacuum conditions at a constant strain rate of 1.6 s^{-1} (Fig. 5b-f). This comparison reveals marked differences in the impact of cell gas across various regions, aligning with theoretical insights from existing literature [10,11].

Comparing the compressive stress–strain curves in Fig. 5a reveals that the influence of cell gas in the linear-elastic region is minor, but becomes more pronounced in the plateau region. The disparity in compressive behavior between vacuum and ambient pressure conditions is evident until the end of the loading cycle at 80% compressive strain. The absence of cell gas significantly reduces the stress required to reach maximum deformation.

The unloading step underscores the substantial impact of cell gas on the recovery behavior of the bead foam. Notably, the slope at the initial phase of the unloading step is markedly influenced by cell gas, indicating that entrapped cell gas functions akin to a spring, facilitating the restoration of the sample. In the latter phase of the unloading step, the residual height of the specimen is closer to the initial height in the presence of cell gas. This observation suggests a potential for improved resistance to long-term cyclic loads of the foam. It indicates that the presence of cell gas plays a key role in recovery. Consequently, it is assumed that cell gas might aid in shape restoration after loading, potentially enabling specifically designed products to better withstand subsequent loads.

Further, we explore the impact of cell gas on crucial parameters. The evaluation of the compression modulus (Fig. 5b) reveals comparable results both under vacuum and ambient conditions. At a strain rate of 1.6 s^{-1}, the compression modulus remains consistent at 9 MPa in both conditions, suggesting that the linear-elastic behavior is dominated by the material composition, here polypropylene (PP). The plateau stress (Fig. 5c) experiences minimal alteration due to the presence of cell gas. Only a slight, non-significant decrease is noted at 4 mbar, as the plateau stress is 0.18 MPa compared to 0.19 MPa under ambient conditions.

The densification strain at 60% compression remains constant, as shown in Fig. 5d. Cell walls undergo substantial deformation and interlocking, reinforcing resistance to deformation in the densification region [23]. Although the impact of cell gas on densification strain is minor, resistance increases with cell gas. Consequently, the stress required to achieve densification is higher with cell gas.

In the specific context of the plateau region, spanning from the plateau stress to the onset of densification, the influence of cell gas becomes pronounced. This influence manifests as a significant reduction in plateau slope (Fig. 5e), declining from 0.56 MPa to 0.35 MPa. This discrepancy can be elucidated by understanding that cell gas plays a stabilizing role on the cells during compression, leading to a more continuous stress decrease. Conversely, at 4 mbar, where cell gas is lacking, deformation occurs at a lower increase in stress up to the densification strain.

The results regarding energy absorption (Fig. 5f) shows changes under vacuum conditions in comparison to ambient pressure. The absorbed energy of the foam up to the densification strain experiences a substantial decrease, transitioning from 0.24 MJ/m^3 at ambient pressure to 0.21 MJ/m^3 at 4 mbar. This observed change in energy absorption is significant for the widespread application as energy absorbers.

3.3. Influence of cell gas on strain rate dependence and recovery behavior of EPP

To delve deeper into the mechanisms influencing the deformation behavior of EPP under normal conditions and at 4 mbar pressure, a series of tests at different strain rates was conducted. The strain rate-dependent behavior is shown in Fig. 6.

In Fig. 6a, the plateau stress remains unaffected in the presence of cell gas, but a non-linear rise is observed with increasing strain rate. This suggests that the increase in plateau stress of EPP is independent of cell gas, attributing the strain rate-dependent behavior to the inherent

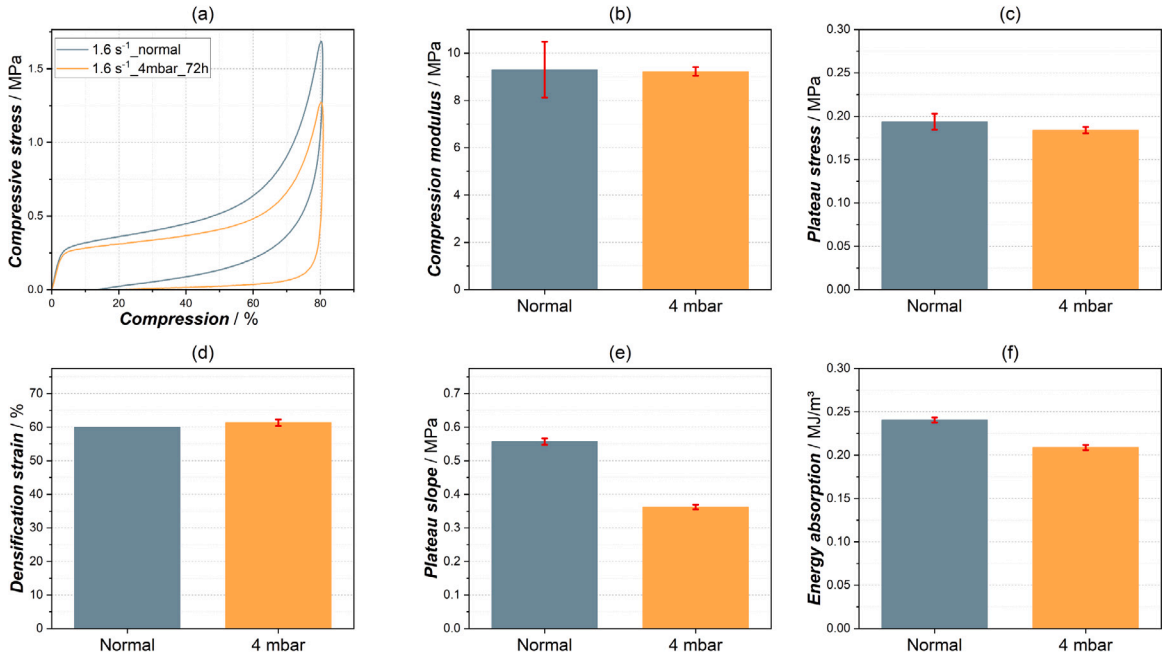

Fig. 5. Visualization of the different mechanical response of EPP with a density of 60 kg/m^3 tested at ambient pressure and 4 mbar at a strain rate of 1.6 s^{-1}: (a) Compression stress–strain curves, (b) compression modulus, (c) plateau stress, (d) densification strain, (e) plateau slope and (f) energy absorption until densification.

material characteristics of the foam. This behavior is in line with Ebert et al. demonstrating a significant dependence of PP on load strain rate [25].

The influence of cell gas on the plateau slope across all three strain rates is particularly interesting. Despite variations in strain rates, the difference between samples tested under ambient pressure and at 4 mbar remains constant. This consistently results in an identical slope of the linear fit for the increase in plateau slope of EPP tested under normal conditions and in vacuum. Consequently, the theory proposed by Bouix et al. [21] does not seem to be applicable in this context; the cell gas is not the primary cause for the strain-dependent rise in resistance against deformation of EPP. This nuanced understanding sheds light on the complex interplay of factors influencing the mechanical behavior of EPP under varying conditions.

To further investigate the recovery behavior of the foams, we closely examined each sample height after compression. In Fig. 6c, one can see how the sample heights changed, 1 min and 72 h after testing, relative to their initial height.

This analysis sheds light on how cell gas continues to affect the recovery of the bead foam. At a strain rate of 0.0016 s^{-1}, just 1 min after testing, samples at ambient pressure showed a Δh of around 15.2%, while those at 4 mbar exhibited a more significant change at 47.5%. This difference is partly due to the non-equilibrium state of the latter samples. After 72 h in ambient conditions, Δh for samples tested at ambient conditions was around 8.2%, whereas for samples tested at 4 mbar, it was 16.2%.

At higher strain rates of 1.6 and 16 s^{-1}, the height reduction stayed the same between 1 min and 72 h in ambient conditions, with a permanent height change of about 5%. In vacuum conditions, while initial height reduction at these higher rates was less than at 0.0016 s^{-1}, the permanent strain consistently stayed around 16% after 72 h.

Regardless of the strain rate, a notable difference of more than 10% in permanent deformation is observed between samples tested under vacuum and ambient conditions. This indicates that cell gas functions as a protective factor during compression, leading to reduced permanent deformation after unloading. This finding suggests that the presence of cell gas in the foam structure plays a key role in minimizing permanent deformation after loading and unloading cycles. This protective mechanism is essential for applications where the resilience and durability of the material are critical, especially in scenarios involving repeated loading and unloading.

4. Conclusions

In this study, a detailed analysis of the mechanical behavior of EPP within a custom-designed vacuum chamber was performed. The innovative approach of comparing the foam behavior at both ambient atmospheric pressure and 4 mbar served as the foundation for our investigations. Prior to studying the influence of cell gas, we determined the necessary evacuation time and assessed evacuation-induced damage. For EPP with a density at 60 kg/m^3, the evacuation conditioning time was 72 h, and no residual damage was detected due to evacuation.

Subsequently the deformation behavior at ambient pressure and 4 mbar was investigated. Minimal influence of cell gas on the linear region was observed, suggesting that the linear-elastic behavior is dominated by the intrinsic material properties of the cell wall material. The base materials behavior also dominates the plateau stress, exhibiting a strain rate-dependent increase independent of cell gas presence.

The plateau slope and energy absorption during the deformation of EPP. Key indicators of the material resistance are highly sensitive to the presence of cell gas. Notably, the observed reduction in plateau slope and energy absorption under vacuum conditions remained consistent across the range of investigated strain rates, from 0.0016 to 16 s^{-1}.

Furthermore, the performed unloading step highlighted the role of cell gas in the recovery behavior of EPP. In the presence of cell gas, recovery was faster and more pronounced. The cell gas acts as a protective factor during compression and resulting in a notable reduction in permanent deformation after unloading. This protective mechanism persisted across different strain rates, emphasizing its significance in preserving the structural integrity of the foam.

In practical terms, these findings have significant implications for applications prioritizing the resilience, durability, and energy absorption of foam materials. The complex influence of cell gas on compression behavior, observed within the controlled setting of the vacuum chamber, enriches our understanding and contributes to a novel and enhanced foam material design for various applications. As a next step, exploring different bead foams will shed light on the influence of the material on cell gas dependence. Additionally, gaining a comprehensive

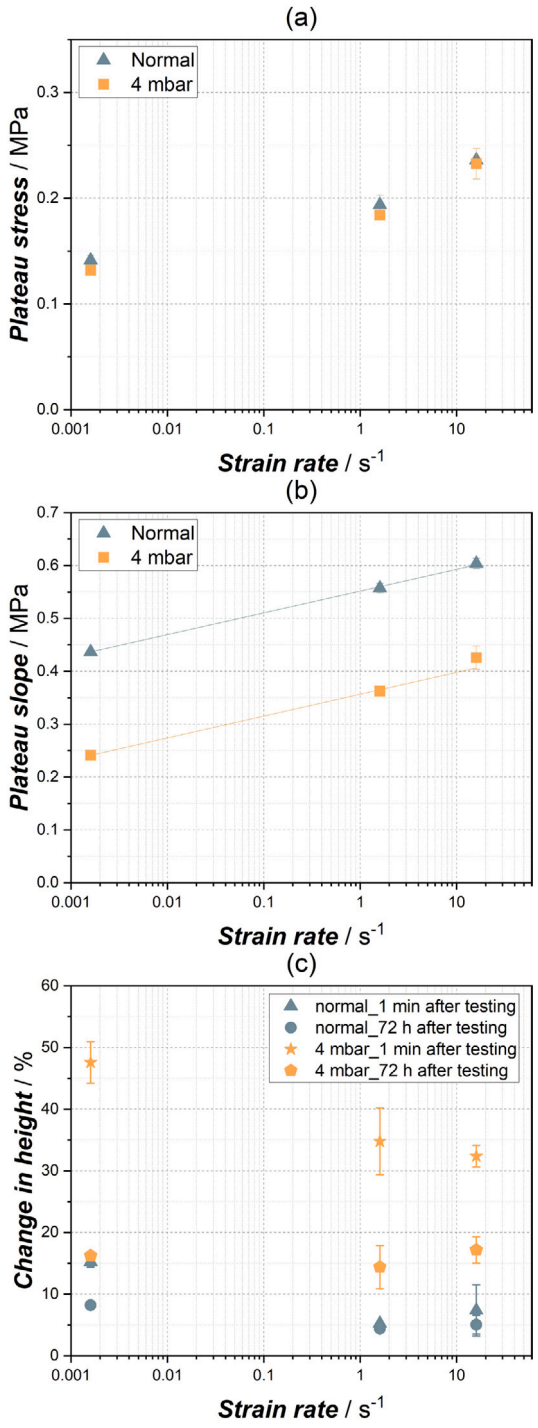

Fig. 6. Strain rate dependence of the plateau stress (a), the plateau slope (b) and the change in height (c) of EPP tested under ambient pressure and at 4 mbar.

perspective requires delving into the long-term cyclic behavior and assessing the impact of cell gas on the fatigue characteristics of these foams. Performing in-situ μCT measurements under both ambient and vacuum pressure conditions will allow to correlate the influence of cell gas on the damage mechanism.

CRediT authorship contribution statement

J. Meuchelböck: Writing – original draft, Visualization, Validation, Methodology, Investigation, Formal analysis, Data curation, Conceptualization. **I. Koch:** Writing – review & editing, Validation, Funding acquisition. **B. Grüber:** Writing – review & editing, Writing – original draft, Validation, Funding acquisition. **M. Müller-Pabel:** Writing – review & editing, Validation, Funding acquisition. **M. Gude:** Writing – review & editing, Validation, Funding acquisition. **H. Ruckdäschel:** Writing – review & editing, Validation, Supervision.

Declaration of competing interest

The authors declare that they have no known competing financial interests or personal relationships that could have appeared to influence the work reported in this paper.

Data availability

Data will be made available on request.

Acknowledgments

The authors would like to thank Alexander Brückner and Michael Groll for inspiration in planning the test set up and the BASF SE for supplying the materials. The work was public funded by the German Research Foundation (Project number: 437872031 - AL474/45-1).

References

[1] N. Weingart, D. Raps, J. Kuhnigk, A. Klein, V. Altstädt, Expanded polycarbonate (EPC)—A new generation of high-temperature engineering bead foams, Polymers (ISSN: 20734360) 12 (10) (2020) 2314, http://dx.doi.org/10.3390/polym12102314, URL https://www.mdpi.com/2073-4360/12/10/2314.

[2] A. Castiglioni, L. Castellani, G. Cuder, S. Comba, Relevant materials parameters in cushioning for EPS foams, Colloids Surf. A (ISSN: 18734359) 534 (March) (2017) 71–77, http://dx.doi.org/10.1016/j.colsurfa.2017.03.049.

[3] A.S.S. Singaravelu, J.J. Williams, P. Shevchenko, J. Ruppert, F. de Carlo, M. Henderson, C. Holmes, N. Chawla, Poisson's ratio of eTPU molded bead foams in compression via in situ synchrotron X-ray microtomography, J. Mater. Sci. (ISSN: 0022-2461) 56 (22) (2021) 12920–12935, http://dx.doi.org/10.1007/s10853-021-06103-w.

[4] P. Rumianek, T. Dobosz, R. Nowak, P. Dziewit, A. Aromiński, Static mechanical properties of expanded polypropylene crushable foam, Materials (Basel, Switzerland) (ISSN: 1996-1944) 14 (2) (2021) http://dx.doi.org/10.3390/ma14020249.

[5] D.T. Morton, A. Reyes, A.H. Clausen, O.S. Hopperstad, Mechanical response of low density expanded polypropylene foams in compression and tension at different loading rates and temperatures, Mater. Today Commun. (ISSN: 23524928) 23 (September 2019) (2020) 100917, http://dx.doi.org/10.1016/j.mtcomm.2020.100917.

[6] A. Reyes, T. Børvik, Quasi-static behaviour of crash components with steel skins and polymer foam cores, Mater. Today Commun. (ISSN: 23524928) 17 (2018) 541–553, http://dx.doi.org/10.1016/j.mtcomm.2018.09.015.

[7] D. Raps, N. Hossieny, C.B. Park, Past and present developments in polymer bead foams and bead foaming technology, Polymer (ISSN: 00323861) 56 (2014) 5–19, http://dx.doi.org/10.1016/j.polymer.2014.10.078.

[8] Mordor Intelligence, Expanded polypropylene (EPP) foam market size & share analysis - growth trends & forecasts (2023 - 2028), 2022, URL https://www.mordorintelligence.com/industry-reports/expanded-polypropylene-epp-foam-market.

[9] E. Linul, P.A. Linul, C. Valean, L. Marsavina, D. Silaghi-Perju, Manufacturing and compressive mechanical behavior of reinforced polyurethane flexible (PUF) foams, IOP Conf. Ser.: Mater. Sci. Eng. 416 (2018) 012053, http://dx.doi.org/10.1088/1757-899X/416/1/012053.

[10] L.J. Gibson, M.F. Ashby, Cellular Solids: Structure and Properties, second ed., Cambridge University Press, ISBN: 9781139878326, 2014, http://dx.doi.org/10.1017/CBO9781139878326.

[11] N.J. Mills, C. Fitzgerald, A. Gilchrist, R. Verdejo, Polymer foams for personal protection: Cushions, shoes and helmets, Compos. Sci. Technol. (ISSN: 02663538) 63 (16) (2003) 2389–2400, http://dx.doi.org/10.1016/S0266-3538(03)00272-0.

[12] N.J. Mills, M.A. Rodriguez-Perez, Modelling the gas-loss creep mechanism in EVA foam from running shoes, Cellular Polym. (ISSN: 0262-4893) 20 (2) (2001) 79–100, http://dx.doi.org/10.1177/026248930102000201.

[13] M.F. Ashby, The properties of foams and lattices, Phil. Trans. R. Soc. A (ISSN: 1364503X) 364 (1838) (2006) 15–30, http://dx.doi.org/10.1098/rsta.2005.1678.

[14] T.M. Gebhart, D. Jehnichen, R. Koschichow, M. Müller, M. Göbel, V. Geske, M. Stegelmann, M. Gude, Multi-scale modelling approach to homogenise the mechanical properties of polymeric closed-cell bead foams, Internat. J. Engrg. Sci. (ISSN: 00207225) 145 (2019) 103168, http://dx.doi.org/10.1016/j.ijengsci.2019.103168.

[15] J. Kuhnigk, T. Standau, D. Dörr, C. Brütting, V. Altstädt, H. Ruckdäschel, Progress in the development of bead foams – A review, J. Cellular Plast. (ISSN: 15307999) (2022) http://dx.doi.org/10.1177/0021955X221087603, 0021955X2210876.

[16] C. Brütting, T. Standau, J. Meuchelböck, P. Schreier, H. Ruckdäschel, A review on semi-crystalline polymer bead foams from stirring autoclave: Processing and properties, E-Polymers (ISSN: 16187229) 23 (1) (2023) http://dx.doi.org/10.1515/epoly-2023-0092.

[17] J. Meuchelböck, D. Raps, A. Brückner, V. Altstädt, H. Ruckdäschel, Flexural fatigue behaviour and damage mechanism of polystyrene bead foams—Influence of the foam density, Int. J. Fatigue (ISSN: 01421123) (2023) 108095, http://dx.doi.org/10.1016/j.ijfatigue.2023.108095.

[18] I. Beverte, Deformation of polypropylene foam Neopolen\textregistered P in compression, J. Cellular Plast. (ISSN: 15307999) 40 (3) (2004) 191–204, http://dx.doi.org/10.1177/0021955X04043718.

[19] P. Viot, D. Bernard, E. Plougonven, Polymeric foam deformation under dynamic loading by the use of the microtomographic technique, J. Mater. Sci. (ISSN: 15734803) 42 (17) (2007) 7202–7213, http://dx.doi.org/10.1007/s10853-006-1422-8.

[20] P. Viot, Hydrostatic compression on polypropylene foam, Int. J. Impact Eng. (ISSN: 0734743X) 36 (7) (2009) 975–989, http://dx.doi.org/10.1016/j.ijimpeng.2008.11.010.

[21] R. Bouix, P. Viot, J.L. Lataillade, Polypropylene foam behaviour under dynamic loadings: Strain rate, density and microstructure effects, Int. J. Impact Eng. (ISSN: 0734743X) 36 (2) (2009) 329–342, http://dx.doi.org/10.1016/j.ijimpeng.2007.11.007.

[22] I. Koch, G. Preiß, M. Müller-Pabel, B. Grüber, J. Meuchelböck, H. Ruckdäschel, M. Gude, Analysis of density-dependent bead and cell structure of expanded polypropylene bead foams from X-ray computed tomography of different resolution, J. Cellular Plast. (ISSN: 15307999) 59 (2) (2023) 165–184, http://dx.doi.org/10.1177/0021955X231165343.

[23] Q.M. Li, I. Magkiriadis, J.J. Harrigan, Compressive strain at the onset of densification of cellular solids, J. Cellular Plast. (ISSN: 15307999) 42 (5) (2006) 371–392, http://dx.doi.org/10.1177/0021955X06063519.

[24] R.Q. Albuquerque, J. Meuchelböck, H. Ruckdäschel, A unified approach for evaluating mechanical compression tests for polymer bead foams, J. Polym. Sci. (ISSN: 2642-4150) (2023) http://dx.doi.org/10.1002/pol.20230704.

[25] C. Ebert, W. Hufenbach, A. Langkamp, M. Gude, Modelling of strain rate dependent deformation behaviour of polypropylene, Polym. Test. (ISSN: 01429418) 30 (2) (2011) 183–187, http://dx.doi.org/10.1016/j.polymertesting.2010.11.011.